

Interdiffusion of solid iron and nickel at high pressure

Molly L. Yunker¹, James A. Van Orman^{*}

Department of Geological Sciences, Case Western Reserve University, Cleveland, OH 44106, USA

Received 7 August 2006; received in revised form 3 November 2006; accepted 18 November 2006

Available online 9 January 2007

Editor: G.D. Price

Abstract

Interdiffusion rates in solid (fcc) iron–nickel alloys have been measured at pressures between 1 and 23 GPa and temperatures between 1423 and 1973 K. The experiments were performed using piston cylinder and multianvil devices, with diffusion couples comprising pure iron and nickel rods placed end to end. Concentration profiles in quenched samples were measured by electron microprobe, and interdiffusion coefficients were determined using the Boltzmann–Matano method. Over the entire range of pressure and temperature studied, interdiffusion coefficients in the iron-rich alloys are described well by a simple exponential function of the homologous temperature, $D = D_0 \exp(-20.4T_m/T)$, where T_m is the melting temperature of the alloy at the pressure of interest and D_0 is a constant equal to $2.7 \times 10^{-4} \text{ m}^2/\text{s}$. These data are consistent, within an order of magnitude, with data for other close-packed (fcc and hcp) metals at the same homologous temperatures. At the conditions of Earth's inner core, diffusion coefficients are predicted to be too small for bulk diffusive exchange between the inner and outer core to be significant. It is thus reasonable to model the chemical evolution of the outer core under the assumption that crystallization of the inner core is a perfect fractional process.

© 2006 Elsevier B.V. All rights reserved.

Keywords: inner core; diffusion; viscosity; iron; nickel; metal; high pressure

1. Introduction

Iron–nickel alloys are the principal constituents of planetary cores, and their chemical diffusion properties are important for understanding physical and chemical processes in planetary interiors. Diffusion is the rate-limiting step in creep of solid metal alloys [1], and is thus important for understanding the viscosity of Earth's inner core [2]. The cooling rates of meteorite parent

bodies are inferred from diffusion profiles, primarily Fe–Ni, preserved in meteorites containing iron-rich metal [3,4]. The chemical evolution of Earth's outer core, which is important for understanding possible core signatures found in some ocean island basalts [5–7], depends on chemical fractionations associated with crystallization of the inner core, and the rate of solid-state diffusion is an important control on the style of the fractionation.

Because the cores of planetary bodies are under extreme pressures, up to 364 GPa at Earth's center, it is necessary to understand the effect of pressure on diffusion rates in Fe–Ni alloys. Diffusion coefficients in liquid iron have been determined experimentally at pressures up to 20 GPa [8], and have been calculated

^{*} Corresponding author.

E-mail addresses: yunker@umich.edu (M.L. Yunker), james.vanorman@case.edu (J.A. Van Orman).

¹ Now at School of Education, University of Michigan, Ann Arbor, MI 48109, USA.

from *ab initio* molecular dynamics simulations at pressures relevant to Earth's outer core [9]. In solid alloys, Fe–Ni interdiffusion coefficients have been measured at pressures up to 4 GPa [10], and diffusion coefficients of some siderophile elements have been determined at pressures up to 20 GPa [11].

Here, new data are presented on rates of Fe–Ni interdiffusion in solid alloys at pressures up to 23 GPa, extending the pressure range over which interdiffusion data have been determined by nearly a factor of six. These pressures approach those within the cores of Mercury and Mars, but are an order of magnitude short of pressures in Earth's inner core. Thus, an important aspect of our study is to evaluate methods used to extrapolate diffusion data to high pressures.

The diffusion coefficient varies as an exponential function of pressure and temperature:

$$D = D_0 \exp[-(E + PV)/RT] \quad (1)$$

where D_0 is a frequency factor, R is the universal gas constant, P is pressure and T is absolute temperature. For metals in which diffusion occurs by an intrinsic vacancy mechanism (i.e. where vacancy formation is thermally activated) the activation energy E represents a sum of the energy of formation and migration of vacancies, and likewise the activation volume V represents a sum of the formation and migration volumes. At moderate pressures the activation volume is usually found to be constant, but V is generally expected to decrease under significant compression. Such a decrease in V with pressure has been documented in highly compressible solid sodium [12] and has been calculated from first principles for Mg and O self-diffusion in MgO at pressures beyond 20 GPa [13].

A simple expression that implicitly accounts for the pressure dependence of diffusion, and the change in activation volume with pressure, is the homologous temperature relation:

$$D = D_0 \exp(-gT_m/RT), \quad (2)$$

where T_m is the melting temperature and g is an empirical constant. This is a convenient relation for pressure extrapolation, since all that is required is knowledge of the homologous temperature, T/T_m , at a given pressure, once g and D_0 have been determined. The homologous temperature relation has been found to provide a good description of experimental diffusion data for a broad range of metals and alloys over a moderate range of pressures, but has only been tested up to ~ 4 GPa [14,15]. Models based on the elastic strain energy involved in vacancy formation and motion have

also been used for high-pressure extrapolation of diffusion data [15], but these models are not easily applied to close-packed (fcc and hcp) iron or iron–nickel alloys because the pressure and temperature derivatives of the elastic constants are not well known.

It is important to note that the alloys in these experiments have the face-centered cubic (fcc) structure, while the phase thought to be stable in the inner core is hexagonally close-packed (hcp). In general, fcc and hcp metals with a wide range of physical and chemical properties are found to have similar diffusion properties when compared at a common homologous temperature [14], but it is not known whether this is true for iron–nickel alloys at very high pressures.

2. Experimental methods and analyses

Fe–Ni interdiffusion coefficients were measured in high pressure experiments in which pure Fe (99.995%) and pure Ni (99.999%) wires, each mirror polished on one side, were placed end-to-end and heated at constant temperature and pressure for a certain period of time. Experiments were performed using a multianvil apparatus for experiments at 12 and 23 GPa, and a piston cylinder device for 1 GPa experiments, both located at the Geophysical Laboratory. Diffusion profiles in quenched samples were measured using an electron microprobe, and interdiffusion coefficients, which vary significantly with concentration, were determined by Boltzmann–Matano analysis [16].

2.1. Multianvil sample assembly

Each multianvil experiment consisted of an MgO octahedron with 8 mm edge length containing an Fe–Ni diffusion couple at its center (Fig. 1A). The multianvil assembly is similar to that described in detail by Bertka and Fei [17]. The unannealed diffusion couple was made from 1 mm diameter pieces of Fe and Ni wire placed end-to-end inside an alumina (Al_2O_3) sleeve with a total length of ~ 1.4 mm. The diffusion couple was carefully placed so that the Fe–Ni interface and thermocouple junction were both within the ~ 1 mm long [18] hotspot at the center of the assembly. Temperature was monitored with a W5%Re/W26%Re thermocouple inserted axially within the cylindrical rhenium heater enclosing the sample assembly, and was separated from the diffusion couple by a thin layer of MgO powder. The uncertainty in the temperature measurement is estimated to be 20 K.

Samples were compressed to the final run pressure at room temperature, at approximately 1 GPa per hour, and

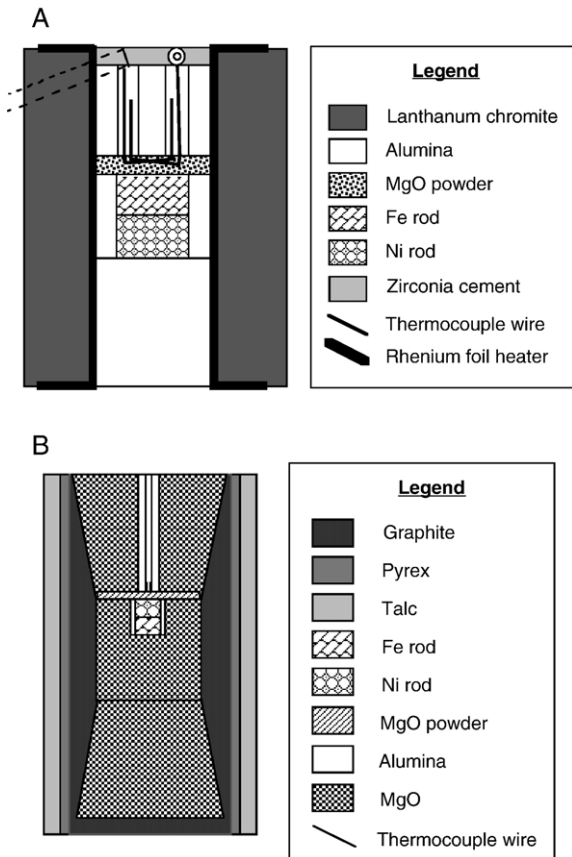


Fig. 1. Schematic representation of (A) cylindrical insert used for the 8/3 multianvil assembly, and (B) piston cylinder assembly, showing Fe–Ni diffusion couple at the center.

then heated at 100 K/min to the run temperature. Experiments were held at constant temperature and pressure for times ranging from 30 min to 10 h and quenched by shutting off the power, cooling to less than 150 °C within 2 s. Following the quench, the sample was ground perpendicular to the diffusion interface, mounted in epoxy, and further ground to a position near the center of the diffusion couple. The sample was then polished with diamond suspensions, to 0.3 μm , and coated with carbon for electron microprobe analysis.

2.2. Piston cylinder sample assembly

Piston cylinder experiments were performed using a 19 mm talc–Pyrex sample assembly with a tapered graphite heater (Fig. 1B). Diffusion couples were constructed as described above and each was placed into a small hole drilled into the center of a cylindrical MgO end piece. MgO powder was packed on top of the diffusion couple to separate it from the W5%Re/W26%

Re thermocouple. The hotspot in a similar piston cylinder assembly with a stepped graphite furnace is approximately 1 cm long [19]. Although the thermocouple junction and sample were not placed at the center of the assembly (Fig. 1B), both were well within the hotspot of the furnace and were separated by a few millimeters at most. Based on temperature profiles measured in similar assemblies [19], the variation in temperature between the thermocouple junction and center of the diffusion couple is expected to have been less than 10 K. Samples were compressed at room temperature, heated at 100 K/min to the final run temperature, and held isothermally for 2 to 18 h. After quenching the run by shutting off the power, the diffusion couple was extracted from the MgO, ground perpendicular to the diffusion interface to reveal the diffusion couple, mounted in epoxy, polished to 0.3 μm with diamond suspensions and carbon-coated for electron microprobe analysis.

2.3. Electron microprobe analysis

The samples were analyzed for Fe and Ni concentrations using the JEOL-JXA-8900 electron microprobe located at the Geophysical Laboratory, Carnegie Institution of Washington. A series of spot analyses were acquired along a line perpendicular to the diffusion interface, avoiding pits or scratches that resulted from polishing. The traverses started and ended at locations that consisted of pure Fe or Ni. Line scans were between 90 and 783 μm long, and spacing between adjacent spots was between 3 and 8 μm . The electron beam had an effective diameter of $\sim 1 \mu\text{m}$, so there was no significant overlap between adjacent analyses. The probe current used was 30 nA, and the accelerating voltage was 15 kV. Rhenium was included in some of the analyses to check for possible contamination from the heater and/or thermocouple, but was not detected. Analyses were considered acceptable if the concentrations of Fe and Ni summed to between 98.5 and 101.5 at.%. The error in Fe and Ni concentrations for each point along the line scan, determined from counting statistics, was less than 0.16% relative between 3 and 97 at.% Fe.

2.4. Grain boundary diffusion?

The starting materials in our experiments were polycrystalline and underwent phase transformations during compression and/or heating, and during quenching and decompression. Thus it is important to evaluate whether diffusion along grain boundaries may have

contributed significantly to bulk diffusive transport in our experiments. Whether grain boundary diffusion is significant depends on the grain size at the conditions of the experiment and the relative mobility of atoms in the crystal lattice and disordered grain boundary region. The effective diffusion coefficient for a polycrystalline material is [1]:

$$D_{\text{eff}} = D_v + \frac{\pi\delta}{d} D_b \quad (3)$$

where D_v is the volume diffusion coefficient, D_b is the boundary diffusion coefficient, δ is the effective width of the grain boundary and d is the grain size. Because the estimated uncertainty in D in our experiments is about a factor of 2 (see below), we consider grain boundary diffusion to make a discernable contribution to bulk transport when $D_{\text{eff}}/D_v > 2$. At atmospheric pressure and temperatures of 0.8 to $0.97T_m$, encompassing the range of homologous temperatures in our experiments, $D_v/(\delta D_b)$ in γ -iron, nickel and other face-centered cubic metals is $\sim 3 \times 10^4$ to 3×10^5 [1]. Thus we expect grain boundary diffusion to be significant only when the grain size is less than $\sim 10 \mu\text{m}$, for the highest homologous temperature experiments, and less than $\sim 100 \mu\text{m}$ for the lowest homologous temperature experiments.

Polished run products and starting materials (consisting of pure bcc-Fe and fcc-Ni wires) were etched in nital (5% nitric acid in ethanol) in an attempt to characterize the initial and final grain sizes. The starting materials consisted of grains that were elongated along the axis of the wire, with widths of approximately $1 \mu\text{m}$. In the run products, the primary grain structure was obscured by fine-scale textures that we interpret to result from phase transitions (including Fe–Ni exsolution) during quenching of the samples. What appeared to be primary grain boundaries could be detected in only one sample, which had been annealed at $1280 \text{ }^\circ\text{C}$ and 1 GPa for 6 h. The grains in the Fe-rich portion of this sample were equant (the Ni-rich portion was too strongly dissolved by the nital to be observed) and the average distance between grain boundaries was $200 \mu\text{m}$, corresponding to an average grain size of $\sim 300 \mu\text{m}$ [20].

Grain growth in metals follows a relationship of the form:

$$D^n - D_0^n = kt \exp(-bT_m/T) \quad (4)$$

where D is the grain diameter at time t , D_0 is the original grain diameter, k is a rate constant, and b and n are non-dimensional constants. The exponent n

usually has a value near 2.5 for fcc metals [21]. Taking a value b of 8.34, derived from grain growth experiments on steel [22], assuming $n=2.5$ and initial grain size D_0 very small, the rate constant implied by this experiment is $1.1 \times 10^{-9} \text{ m}^{2.5}/\text{s}$. We used Eq. (2) to simulate grain growth during the initial heating and isothermal annealing of our diffusion couples. In all but one case we found that by the end of the initial heating stage the grain size would already have exceeded the critical value at which the contribution of grain boundary diffusion becomes insignificant. This indicates that in all but one experiment the effects of grain boundary diffusion need only be considered during the initial heating. To assess the extent of transport during heating we performed a “zero-time” experiment at 12 GPa, in which the sample was heated to $1500 \text{ }^\circ\text{C}$, then immediately quenched. The Fe–Ni profile in the recovered sample was less than $10 \mu\text{m}$ long, one to two orders of magnitude shorter than any of the experimental diffusion profiles. We made no attempt to correct for this minor pre-anneal diffusive transport, since doing so would not change any of the diffusion coefficients by more than 20%.

In one low temperature experiment (#431, at $0.8T_m$) our grain growth simulations indicate that the grain size would not have reached the critical value of $100 \mu\text{m}$ during the initial heating, but rather within the first hour of the isothermal diffusion anneal. Because the duration of this experiment was long (18 h) we expect that grain boundary diffusion had at most a modest influence on bulk transport in this experiment.

Further evidence that grain boundary diffusion did not have a significant influence on bulk transport in our experiments comes from our time series experiments, described below. Experiments run at the same conditions (12 GPa, $1600 \text{ }^\circ\text{C}$) between 0.5 and 10 h yielded diffusion coefficients that agreed with each other within a factor of two. Diffusion coefficients were not found to decrease with anneal time, as would be expected if grain boundary diffusion had played an important role.

2.5. Calculation of diffusion coefficients

Diffusion coefficients were calculated using the Boltzmann–Matano method [16], which allows diffusion coefficients to be determined as a function of concentration along the diffusion profile. It was necessary to use this numerical method because no analytical solution to the diffusion equation exists when diffusion coefficients vary strongly with composition, as they do in the Fe–Ni system [10]. The

Boltzmann–Matano equation is derived from Fick’s second law of diffusion,

$$\frac{\partial C}{\partial T} = \frac{\partial}{\partial x} \left(D(C) \frac{\partial C}{\partial x} \right) \quad (5)$$

by combining Boltzmann’s variable transformation with Matano’s geometry [16]. This method relies upon two important assumptions: (1) the diffusion coefficient is only a function of the concentration, and not of position (aside from the dependence due to the change in concentration with position) or time; and (2) the diffusion couple is effectively infinite (i.e. diffusion does not extend to either end of the couple). Both of these conditions are satisfied in these experiments. At the run conditions there are no phase changes that would make the diffusion coefficient a function of position. We do find that the grains coarsen during an experiment, so the diffusion coefficient could change as a function of time as fast grain boundary transport paths are eliminated; however, as discussed above, grain boundary diffusion is not expected to be significant in these experiments, and, as shown below, the diffusion coefficients are found not to vary significantly with time. The Boltzmann–Matano formula for measuring diffusivity as a function of composition is:

$$\tilde{D}(C') = -\frac{1}{2t} \left(\frac{dx}{dC} \right)_{C'} \int_0^{C'} x dC \quad (6)$$

where C' is the concentration of Fe or Ni at a certain point along the diffusion profile, t is the time that the diffusion couple was held at high temperature, and dx/dC represents the slope at a certain composition, C' . The integral in Eq. (4) was calculated numerically using the Riemann sum rule [23]. The plane $x=0$, often called the Matano interface, is positioned such that

$$\int_0^{C^0} x dC = 0 \quad (7)$$

and represents the plane in which an equal number of atoms have crossed in both directions (here C^0 refers to pure Fe, or pure Ni). To find the slope of the tangent line, dx/dC , at a given concentration, it is necessary to fit a curve to the data. The appropriate functional form for the curve is not known *a priori*. We fit a polynomial to the inverse error function of the concentration data versus distance, rather than to the raw concentration data (Fig. 2), because this was found to yield a much better fit to the data with a lower order polynomial.

By using the Boltzmann–Matano method, we have made the assumption that the molar volumes of Fe

and Ni are equal, and that there is no variation in molar volume with composition [10]. Iron and nickel have similar but not identical molar volumes; therefore on one profile we used the Balluffi [24] correction to the Boltzmann–Matano method to account for the differences in molar volumes of Fe and Ni. The Balluffi equation for the interdiffusion coefficient is:

$$\tilde{D} = -\frac{1}{2t} \frac{dx}{dC_1} \left\{ [1 - C_1(V_1 - V_2)] \int_{C_1(-\infty)}^{C_1(x)} x dC_1 + V_2 C_1 \int_{C_1(-\infty)}^{C_1(x)} \left(\frac{V_1 - V_2}{V_2} \right) x dC_1 \right\}$$

where C_1 is the concentration of Fe in mol/m³, V_1 is the molar volume of Fe (7.27 cm³/mol at 1 atm), and V_2 is the molar volume of Ni (6.59 cm³/mol). Diffusion coefficients determined using Balluffi’s equation differed from those determined using the standard Boltzmann–Matano method by less than 10%, and in most cases less than 1%. These errors are so small that we considered it unnecessary to use Balluffi’s correction.

3. Results

Diffusion profiles for experiments run at 1, 12, and 23 GPa are shown in Fig. 3. In all experiments, the Matano interface (at $x=0$) is located at an Fe concentration of 40 ± 2 at.%. All diffusion profiles are asymmetric, regardless of pressure, temperature or time, with shallower slopes on the Ni-rich side indicating

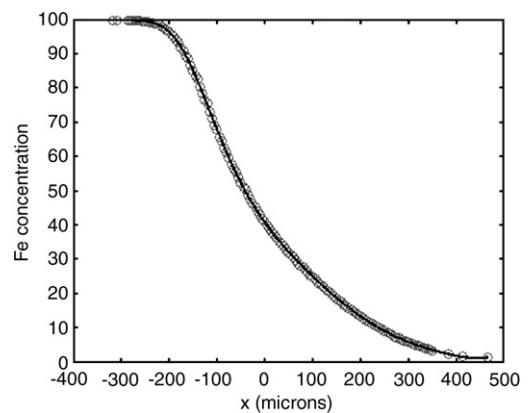


Fig. 2. Typical diffusion profile (from Expt #490) showing Fe concentration versus distance, and a curve fit to the data to determine the slope at each point. A polynomial, in this case 9th order, was fit to the inverse error function of the concentration data versus distance. The curve shown represents the re-inverted fit to the data at concentrations between 3 and 97 at.% Fe.

higher diffusion rates. The length of the diffusion profiles increases approximately with the square root of the run time at constant temperature and pressure, as expected for lattice diffusion, and increases with temperature at constant pressure and run duration, also as expected for a thermally activated diffusion process.

Table 1 lists the Fe–Ni interdiffusion coefficients determined by the Boltzmann–Matano method for each experiment, at compositions of 90, 50 and 10 at.% Fe. Fig. 4 shows Fe–Ni interdiffusion coefficients for each experiment over a full range of compositions between 3 and 97 at.% Fe. Interdiffusion coefficients could not be determined at compositions approaching pure Ni and pure Fe, because the Boltzmann–Matano method is inaccurate at the tails of diffusion profiles, where dx/dc becomes very large and poorly constrained. Interdiffusion coefficients have approximately the same functional dependence on Fe concentration at every temperature, with interdiffusion coefficients highest in alloys with ~60–90 at.% Ni.

It is difficult to assess rigorously the uncertainty in interdiffusion coefficients determined by the Boltzmann–Matano method. The largest source of uncertainty is in determining dx/dc at the composition of interest. Because the functional form for $D(C)$ is not known in advance there is inevitably some subjectivity in choosing the polynomial fit to the profile, from which the slope at each point is determined. However, a sensitivity analysis shows that the diffusion coefficients do not change significantly with the order of the polynomial fit, as long as the order of the polynomial is high enough to obtain a good visual fit to the profile, but much smaller than the number of data points in the diffusion profile. For example, varying the order of the polynomial fit to the profile shown in Fig. 2 from 7 to 10 leads to a maximum variation of less than 25% in the diffusion coefficient calculated at each point along the profile.

The best measure of the total uncertainty in D is the reproducibility of the experimental data at the same conditions. Three experiments performed at the same pressure and temperature (12 GPa and 1600 °C) yielded diffusion coefficients that had an overall variation of ± 0.36 log units (2σ) at the same composition and did not vary systematically with time (Fig. 5). Thus, we estimate that the diffusion coefficients calculated from the multianvil experiments are reproducible to within approximately a factor of two.

4. Discussion

An important objective of this study is to evaluate the pressure dependence of diffusion rates in iron nickel

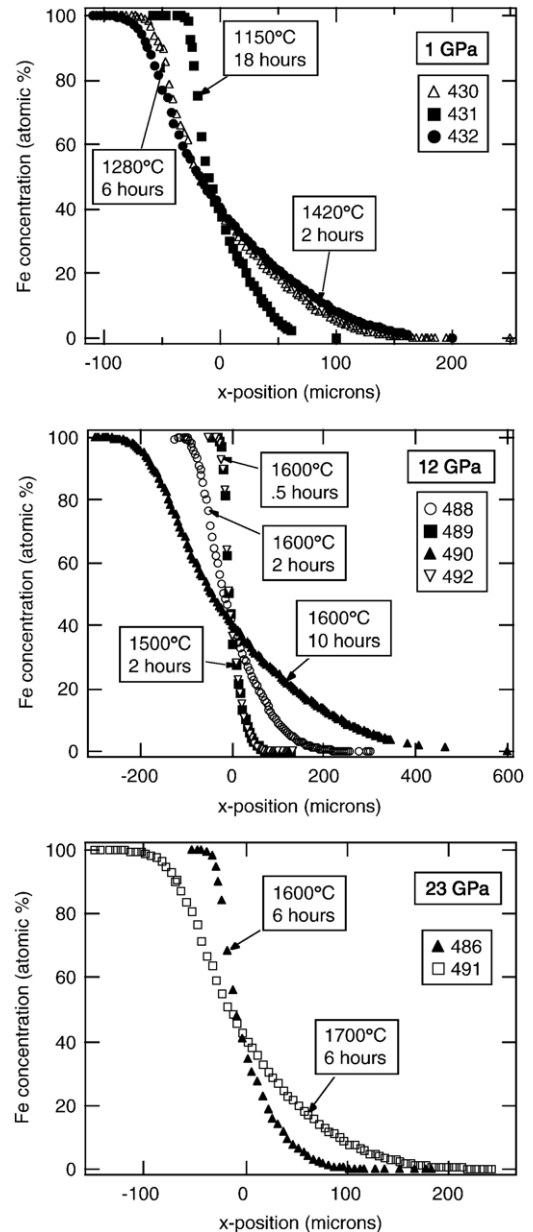


Fig. 3. Diffusion profiles for experiments at 1, 12, and 23 GPa. At the same pressure, it can be seen that diffusion profiles lengthen with time and temperature.

alloys so that data can be extrapolated with more confidence to conditions within the deep interiors of planetary bodies. Here, we focus the discussion on Fe-rich alloys because these are most relevant to planetary cores, and the high-pressure melting behavior is much better known than for Ni-rich alloys. Iron-rich fcc (Fe, Ni) alloys are nearly ideal solutions [25], and differences between iron and nickel intrinsic diffusion coefficients are relatively small [10]. Thus, the interdiffusion co-

Table 1
Summary of experimental conditions and interdiffusion coefficients

	High P device ^a	P (GPa)	T (°C)	t (h)	D (m ² /s) (10 at.% Ni)	D (m ² /s) (50 at.% Ni)	D (m ² /s) (90 at.% Ni)
430	PC	1	1280	6	1.58E–14	4.50E–14	1.13E–13
431	PC	1	1150	18	2.76E–15	1.09E–14	2.77E–14
432	PC	1	1420	2	6.51E–14	2.31E–13	4.27E–13
488	MA	12	1600	2	9.73E–14	2.98E–13	4.63E–13
489	MA	12	1500	2	1.16E–14	1.98E–14	6.01E–14
490	MA	12	1600	10	1.14E–13	3.16E–13	5.51E–13
492	MA	12	1600	0.5	5.13E–14	8.46E–14	2.36E–13
486	MA	23	1600	6	6.83E–15	1.35E–14	3.66E–14
491	MA	23	1700	6	3.84E–14	7.97E–14	1.76E–13

^a PC=piston cylinder, MA=multianvil.

efficients measured in this study on Fe-rich compositions are expected to be approximately equal to Ni self-diffusion coefficients at the same composition [16].

Fig. 6 shows Fe–Ni interdiffusion coefficients as a function of pressure, at 10 at.% Ni, including the results of Goldstein et al. [10] at 1 atm and 4 GPa. The Goldstein et al. results, and our data at 1 GPa, are extrapolated to a common temperature of 1600 °C by fitting the data at each pressure to the Arrhenius relation (Eq. (1)). Based on their results at 1 atm and 4 GPa, Goldstein et al. [10] calculated an activation volume of 6 cm³/mol. Fitting a line to all of the data together, up to 23 GPa, we find a much smaller activation volume of 3.1 ± 0.7 (2σ) cm³/mol. A decrease in activation volume at high pressures is consistent with the homologous temperature scaling, since the slope of the iron melting curve, dT_m/dP, decreases with increasing pressure. This can be seen in the dotted curve in Fig. 6, which represents the homologous temperature extrapolation of the 1 atm Goldstein et al. data, using the high-pressure melting curve of Anderson and Isaak [26] for pure Fe, and assuming that the depression in liquidus temperature on the addition of 10 at.% Ni was 40 K (the same liquidus depression observed at 1 atm [27]). At pressures up to 4 GPa the homologous temperature scaling predicts an activation volume of 4.6 cm³/mol, decreasing to an average value of 3.5 cm³/mol for pressures up to 23 GPa. The predicted change in activation volume with pressure is less than implied by a comparison of the present data set with the Goldstein et al. [10] data set. However, considering the uncertainties in measured diffusion coefficients, the homologous temperature extrapolation predicts the high-pressure diffusion coefficients quite well over the entire pressure range studied.

The homologous temperature relation also describes the temperature dependence of the high-pressure diffusion data with fair accuracy. In Fig. 7, the present

data at 1, 12 and 23 GPa are compared, on an Arrhenius plot, with the predictions of the homologous temperature scaling fitted to the 1 atm Goldstein et al. [10] data. The homologous temperature scaling correctly predicts the data within an order of magnitude at all pressures, but overestimates the activation enthalpy at 1 GPa, and appears to underestimate the activation enthalpy at 12 and 23 GPa. In Fig. 8, the diffusion data at all pressures are shown as a function of T_m/T. Also shown are self-diffusion data for pure Fe and pure Ni with the fcc structure ([14] and references therein). According to the homologous temperature relation, all of the data should collapse onto a common line on this plot. Although there is some scatter, within the mutual uncertainties most of the data are consistent with this relation. A fit to our data yields a homologous temperature expression (Eq. (2)) with g/R=20.4 and D₀=2.7 × 10⁻⁴ m²/s. At 1 atm, this fit corresponds to an activation energy of 300 kJ/mol, which is in good agreement with the value of 318 kJ/mol reported by Goldstein et al. [10]. The value of D₀ is also in good agreement with the value of 5.3 × 10⁻⁴ m²/s reported by Goldstein et al.

Fig. 9 shows that, when the data are interpolated to a constant homologous temperature (in this case T/T_m=0.874, or T_m/T=1.144) there is no significant variation in the diffusion coefficient with pressure. Therefore it appears that the homologous temperature relation is a reasonably accurate method for extrapolating diffusion data in iron–nickel alloys to high pressure, at least up to 23 GPa.

The temperature of Earth's inner core is estimated to be ~0.85–0.95 of the melting temperature for the pure Fe–Ni alloy. Because the slope of the melting curve, dT_m/dP, decreases at high pressure [27,28], the homologous temperature relation predicts that the activation volume for diffusion will decrease significantly at very high pressures. At the conditions of the

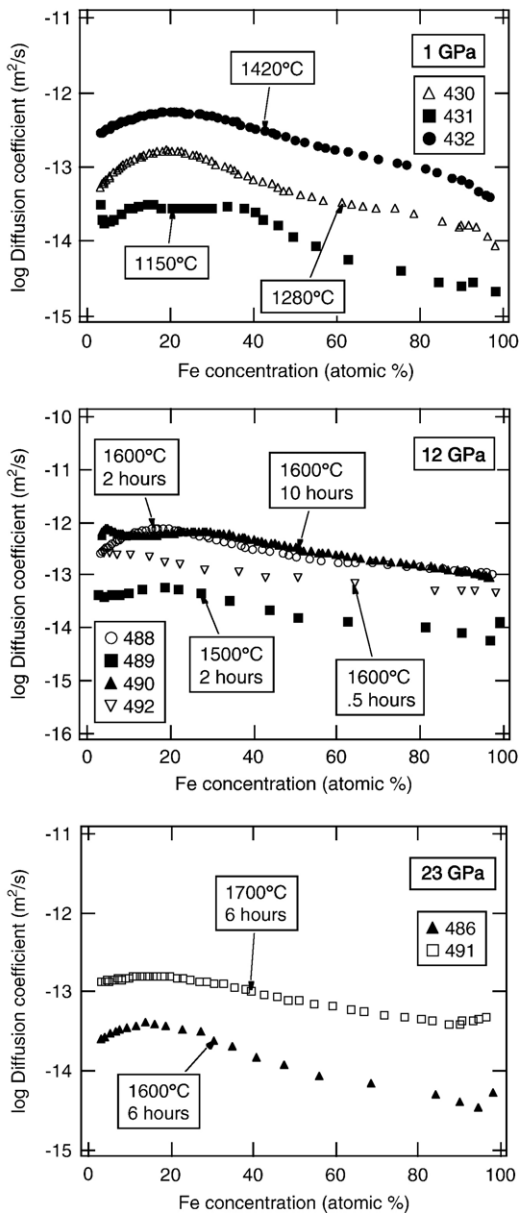


Fig. 4. Interdiffusion coefficients calculated as a function of Fe concentration using the Boltzmann–Matano method, between ~3 and 97 at.% Fe. Diffusion coefficients are highest in alloys with ~60–90 at.% Ni, at all pressures, and lowest in nearly pure Fe.

inner core, the homologous temperature relation predicts diffusion coefficients in the range $4.5 \times 10^{-15} \text{ m}^2/\text{s}$ to $6.6 \times 10^{-14} \text{ m}^2/\text{s}$. If the activation volume is assumed to remain constant at high pressures the diffusion coefficients calculated at inner core conditions are significantly smaller. For example, at conditions near the interface between the inner and outer core, 330 GPa and ~5700 K [29], the interdiffusion coefficient calculated

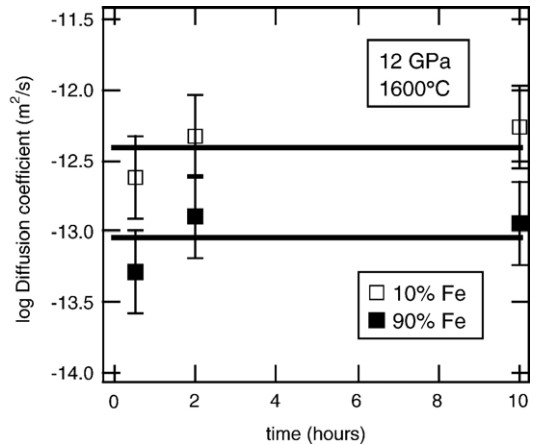


Fig. 5. Results of time series experiments at 12 GPa and 1600 °C. No decrease in diffusion coefficients with time is observed, as would be expected if grain boundary diffusion was significant (due to elimination of grain boundaries during coarsening). The total variation in diffusion coefficients at a given composition is approximately a factor of two.

assuming a constant activation volume of $3.1 \text{ cm}^3/\text{mol}$ is $1.8 \times 10^{-16} \text{ m}^2/\text{s}$. Using the higher activation volume of $6 \text{ cm}^3/\text{mol}$ reported by Goldstein et al. from experiments up to 4 GPa gives a much smaller interdiffusion coefficient of $3 \times 10^{-25} \text{ m}^2/\text{s}$. These large discrepancies in the extrapolated values highlight the importance of the high-pressure extrapolation method. The data presented in this paper provide support for the accuracy of the homologous temperature relation at high pressures; future studies at significantly higher pressures

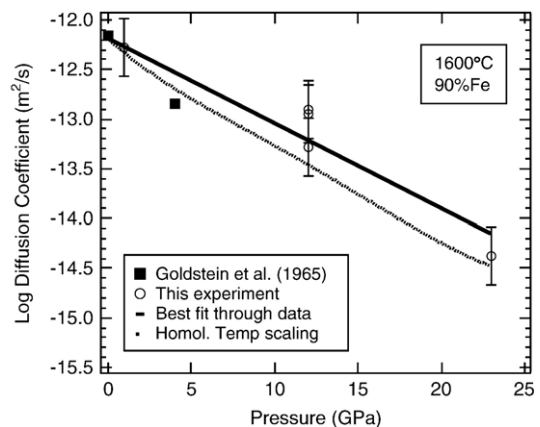


Fig. 6. Diffusion coefficients versus pressure at 1600 °C and 10 at.% Ni. The solid line shows a linear fit to all of the data (including 1 atm and 4 GPa data from Goldstein et al. [10]). The activation volume obtained from this fit is $3.1 \text{ cm}^3/\text{mol}$, much smaller than the value of $6 \text{ cm}^3/\text{mol}$ determined by [10]. The dotted curve shows a homologous temperature extrapolation based only on the 1 atm data of [10].

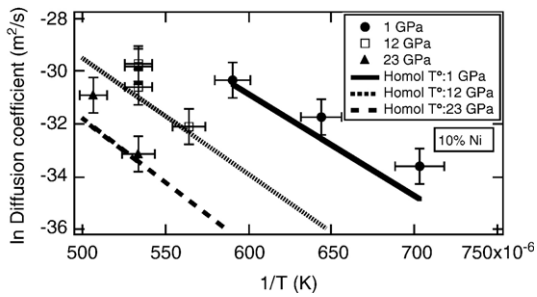


Fig. 7. An Arrhenius plot of the interdiffusion data at 10 at.% Ni. Lines show diffusion coefficients predicted by the homologous temperature relation, fit only to the 1 atm data of Goldstein et al. [10].

and/or on more compressible metals may provide an even more rigorous test of its utility.

5. Applications

Inner core conditions are extreme, and therefore pose a challenge for modeling diffusion-controlled processes in a laboratory setting. However, the experiments designed for this study were successful in determining diffusion coefficients at pressures nearly an order of magnitude higher than have previously been studied in the Fe–Ni system and confirmed the homologous temperature relation as a useful and reasonably accurate method for extrapolating diffusion coefficients to very high pressures. The data collected from these experiments are relevant to materials-based estimates of inner

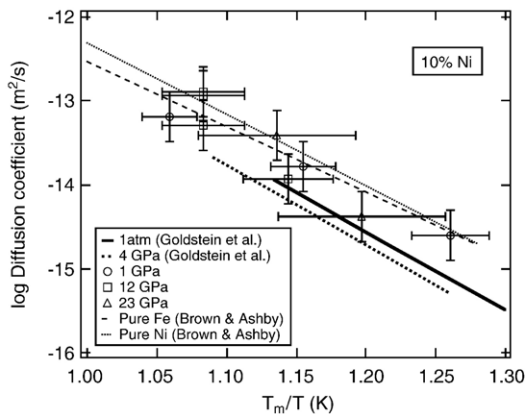


Fig. 8. Diffusion coefficients as a function of T_m/T . The uncertainty in T_m/T reflects a combination of the uncertainty in the experimental temperature and the melting temperature of the alloy at the pressure of the experiment. The uncertainty in T_m was evaluated by considering the variation among three different melting curves for pure Fe [26,28,33], and was estimated as 10 K at 1 GPa, 45 K at 12 GPa and 100 K at 23 GPa. The actual uncertainty is somewhat larger because the influence of 10 at.% Ni on the liquidus temperature has not been determined at high pressures; the depression of the liquidus was assumed equal to that at atmospheric pressure.

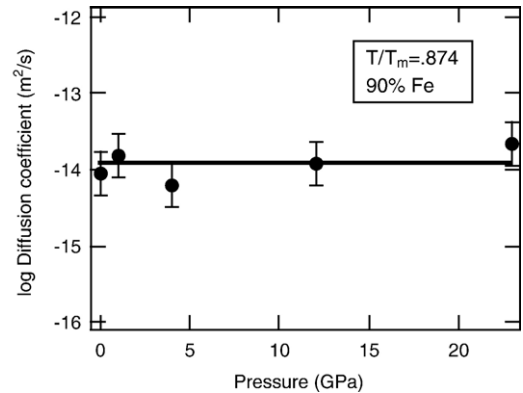


Fig. 9. Diffusion coefficients versus pressure at constant T/T_m , including data from [10]. Within error, the diffusion coefficients remain constant.

core viscosity, and provide constraints on the kinetics of chemical exchange between the inner and outer core.

5.1. Viscosity of the inner core

Van Orman [2] estimated the viscosity of the inner core ($\sim 10^{11}$ Pa s) based on mechanical property data for a variety of metals and minerals and diffusion coefficients estimated for the hcp phase of iron based on a homologous temperature scaling for other hcp metals. The diffusion coefficients determined here for Fe–Ni alloys with the fcc structure are approximately an order of magnitude smaller at the same homologous temperatures. It is not clear whether these data, with the right composition but wrong structure, are preferable to data for hcp metals like zinc and cadmium for estimating the diffusion properties of Earth's inner core. Ultimately we need diffusion data for hcp-Fe itself, although the technical challenges in acquiring these data will be significant. In any case, using the diffusion coefficients determined here for the fcc metal at the appropriate homologous temperature would give a viscosity estimate for Earth's inner core of $\sim 10^{12}$ Pa s, an order of magnitude larger than the previous estimate. These estimates are not particularly satisfactory considering the long extrapolation of the diffusion data, and perhaps more importantly the uncertainty in the creep mechanism at the very low stresses and presumably very large grain sizes of the inner core, but they are the best that can be done with the present data.

5.2. Chemical exchange between the inner and outer core

It has been suggested that the radiogenic Os isotope signatures of some plume basalts reflect a contribution of

outer core material to the plume source [5–7]. The hypothesis is that crystallization of the inner core fractionates Re and Pt from Os, leaving the outer core with relative enrichments in ^{190}Pt and ^{187}Re that evolve over time to radiogenic $^{186}\text{Os}/^{188}\text{Os}$ and $^{187}\text{Os}/^{188}\text{Os}$ ratios. The chemical and isotopic evolution of the outer core has been modeled [7] assuming that crystallization of the inner core is perfectly fractional; i.e. that each increment of solid metal is locally in equilibrium with the liquid outer core as it crystallizes, but that there is no chemical exchange with the liquid following crystallization. This assumption is an important one, because element ratios are modified most efficiently by a fractional process; post-crystallization chemical exchange between the inner and outer core would lead to less radiogenic osmium isotope ratios in the outer core and would place severe constraints on the core interaction models.

The validity of the fractional crystallization assumption depends on the rate of transport in the inner core relative to the rate of inner core growth, and can be evaluated in terms of a non-dimensional Peclet number, $Pe = Vl/D$, where V is the rate of inner core growth (in m/s), l is the radius of the inner core, and D is the diffusion coefficient. The Peclet number represents the ratio of the characteristic times for crystal growth and diffusion, and crystallization can be considered perfectly fractional if $Pe \gg 1$. The average rate of growth of the inner core is $\sim 10^{-11}$ m/s, assuming it began to grow about 3.5 billion years ago, and the radius is 1220 km. The diffusion coefficients for Re, Os and Pt appear to be somewhat smaller than the Fe–Ni interdiffusion coefficient [30], but even using the diffusion coefficients determined here at the appropriate homologous temperatures ($\sim 0.85\text{--}0.95T_m$) the Peclet number is $\sim 10^8$. Inner core crystallization thus can be safely considered to be a fractional process, and this conclusion holds even if the diffusion coefficient is underestimated by several orders of magnitude. Convection in the inner core has been suggested [31] but would have to be quite vigorous to have a significant influence on chemical exchange with the outer core, given the sluggish diffusion kinetics.

In aqueous and magmatic systems, it has been shown that when diffusion is very slow compared to crystal growth, elements that are adsorbed or enriched at the solid/liquid interface may be trapped within the solid as it grows [32]. Although this scenario has not, to our knowledge, been considered previously in the context of inner core growth, it is worth considering briefly since it has the potential to lead to anomalous chemical fractionation. Whether adsorption effects are significant

can be evaluated in terms of the Peclet number discussed above, but in this case with the relevant length scale being the half-thickness of the adsorption layer. Because this layer is unlikely to exceed a few nanometers in thickness [31], the Peclet number is expected to be 10^{-6} or less. Since the Peclet number must be greater than ~ 0.1 for adsorption effects to be significant [31], adsorption effects do not need to be considered for chemical exchange during inner core growth.

6. Conclusions

Interdiffusion coefficients for solid Fe–Ni alloys with the fcc structure were successfully determined at pressures up to 23 GPa, a factor of six higher than previous diffusion studies on this system. While these pressures are an order of magnitude lower than pressures within Earth's inner core, this study provides an improved base for extrapolating diffusion data, and diffusion-related properties such as viscosity, to higher pressures.

The interdiffusion coefficients in iron-rich alloys at all pressures and temperatures considered in this study can be described by a simple function of the homologous temperature, $D = D_0 \exp(-20.4T_m/T)$, where T_m is the melting temperature of the alloy at the pressure of interest and D_0 is a constant equal to 2.7×10^{-4} m²/s. The alloys in these experiments had the fcc structure, in contrast to the hcp structure thought to be stable in Earth's inner core, but the results are similar, within an order of magnitude, to diffusion data for other close-packed (fcc and hcp) metals when compared at the same homologous temperatures. Thus, this expression can be used, with caution, to estimate diffusion coefficients in Earth's inner core. For values of T/T_m in the range 0.85–0.95, the Fe–Ni interdiffusion coefficient is predicted to be between 4.5×10^{-15} m²/s and 6.6×10^{-14} m²/s. These diffusion coefficients are small enough to prohibit significant diffusive chemical exchange between the inner and outer core, and imply that the chemical evolution of the outer core can be modeled assuming perfectly fractional inner core crystallization.

Acknowledgements

The experiments and analyses reported in this paper were performed at the Geophysical Laboratory, Carnegie Institution of Washington. We thank Yingwei Fei for his advice in operating the multianvil apparatus, Chris Hadidiacos and Nancy Chabot for assistance with the electron microprobe, and two anonymous reviewers for valuable comments that helped improve the presentation

of the manuscript. This material is based upon work supported by the National Science Foundation under grant no. 0322766 (JV).

References

- [1] H.J. Frost, M.F. Ashby, *Deformation-Mechanism Maps*, Pergamon Press, Oxford, 1982.
- [2] J.A. Van Orman, On the viscosity and creep mechanism of Earth's inner core, *Geophys. Res. Lett.* 31 (2004) L20606.
- [3] V. Saikumar, J.I. Goldstein, An evaluation of the methods to determine the cooling rates of iron meteorites, *Geochim. Cosmochim. Acta* 52 (1988) 715–726.
- [4] W.D. Hopfe, J.I. Goldstein, The metallographic cooling rate method revised: application to iron meteorites and mesosiderites, *Meteorit. Planet. Sci.* 36 (2001) 135–154.
- [5] R.J. Walker, J.W. Morgan, M.F. Horan, Osmium-187 enrichment in some plumes: evidence for core–mantle interaction? *Science* 269 (1995) 819–822.
- [6] A.D. Brandon, R.J. Walker, J.W. Morgan, M.D. Norman, H.M. Prichard, Coupled ^{186}Os and ^{187}Os evidence for core–mantle interaction, *Science* 280 (1998) 1570–1573.
- [7] A.D. Brandon, R.J. Walker, I.S. Puchtel, H. Becker, M. Humayun, S. Revillon, ^{186}Os ^{187}Os systematics of Gorgona Island komatiites: implications for early growth of the inner core, *Earth Planet. Sci. Lett.* 206 (2003) 411–426.
- [8] D.P. Dobson, Self-diffusion in liquid Fe at high pressure, *Phys. Earth Planet. Inter.* 130 (2002) 271–284.
- [9] D. Alfè, G. Kresse, M.J. Gillan, Structure and dynamics of liquid iron under Earth's core conditions, *Phys. Rev., B* 61 (2000) 132–142.
- [10] J.I. Goldstein, R.E. Hanneman, R.E. Ogilvie, Diffusion in the Fe–Ni system at 1 atm and 40 kbar pressure, *Trans. AIME* 233 (1965) 812–820.
- [11] H.C. Watson, Y. Fei, E.B. Watson, Diffusion of siderophile elements in iron–nickel alloys at high pressure and temperature, *Lunar Planet. Sci. Conf.* 34 (2003) 1871.
- [12] N.H. Nachtrieb, J.A. Weil, E. Catalano, A.W. Lawson, Self-diffusion in solid sodium. II. The effect of pressure, *J. Chem. Phys.* 20 (1952) 1189–1194.
- [13] J. Ita, R.E. Cohen, Effects of pressure on diffusion and vacancy formation in MgO from non-empirical free-energy integrations, *Phys. Rev. Lett.* 79 (1997) 3198–3201.
- [14] A.M. Brown, M.F. Ashby, Correlations for diffusion constants, *Acta Metall.* 28 (1980) 1085–1101.
- [15] C.G. Sammis, J.C. Smith, G. Schubert, A critical assessment of estimation methods for activation volume, *J. Geophys. Res.* 86 (1981) 10707–10718.
- [16] P.G. Shewmon, *Diffusion in Solids*, 2nd edition, The Minerals, Metals, & Materials Society, 1998.
- [17] C.M. Bertka, Y. Fei, Mineralogy of the Martian interior up to core–mantle boundary pressures, *J. Geophys. Res.* 102 (1997) 5251–5264.
- [18] W. van Westrenen, J.A. Van Orman, H. Watson, Y. Fei, E.B. Watson, Assessment of temperature gradients in multianvil assemblies using spinel layer growth kinetics, *Geochem. Geophys. Geosyst.* 4 (4) (2003) 1036–1045.
- [19] E.B. Watson, D.A. Wark, J.D. Price, J.A. Van Orman, Mapping the thermal structure of solid-media pressure assemblies, *Contrib. Mineral. Petrol.* 142 (2002) 640–652.
- [20] M.I. Mendelson, Average grain size in polycrystalline ceramics, *J. Am. Ceram. Soc.* 52 (1969) 443–446.
- [21] D.J. Humphreys, M. Hatherly, *Recrystallization and Related Annealing Phenomena*, Pergamon Press, New York, 1995, 497 pp.
- [22] D.G. Cole, P. Feltham, E. Gillam, On the mechanism of grain growth in metals, with special reference to steel, *Proc. Phys. Soc. B* 67 (1954) 131–137.
- [23] J. Stewart, *Calculus*, 4th Edition, Brooks/Cole Publishing Company, California, 1999, 1185 pp.
- [24] R.W. Balluffi, On the determination of diffusion coefficients in chemical diffusion, *Acta Metall.* 8 (1960) 871–873.
- [25] W. Rammensee, D.G. Fraser, Activities in solid and liquid Fe–Ni and Fe–Co alloys determined by Knudsen cell mass spectrometry, *Ber. Bunsenges Phys. Chem.* 85 (1981) 588–592.
- [26] O.L. Anderson, D.G. Isaak, Calculated melting curves for phases of iron, *Am. Mineral.* 85 (2000) 376–385.
- [27] L.J. Swartzendruber, V.P. Itkin, C.B. Alcock, *Phase Diagrams of Binary Iron Alloys: Fe–Ni (Iron–Nickel)*, ASM International, 1993, pp. 256–278.
- [28] Y. Ma, M. Somayazulu, G. Shen, H. Mao, J. Shu, R.J. Hemley, In situ X-ray diffraction studies of iron to Earth-core conditions, *Phys. Earth Planet. Inter.* 143–144 (2004) 455–467.
- [29] G. Steinle-Neumann, L. Stixrude, R.E. Cohen, O. Gulseren, Elasticity of iron at the temperature of the Earth's inner core, *Nature* 413 (2001) 57–60.
- [30] H.C. Watson, E.B. Watson, Siderophile trace element diffusion in Fe–Ni alloys, *Phys. Earth Planet. Inter.* 139 (2003) 65–75.
- [31] R. Jeanloz, H.-R. Wenk, Convection and anisotropy of the inner core, *Geophys. Res. Lett.* 15 (1988) 72–75.
- [32] E.B. Watson, Surface enrichment and trace-element uptake during crystal growth, *Geochim. Cosmochim. Acta* 60 (1996) 5013–5020.
- [33] H.M. Strong, F.P. Bundy, Fusion curves of four group VIII metals to 100000 atmospheres, *Phys. Rev.* 115 (1959) 278–284.